ABCM Symposium Series in Mechatronics - Vol. 2 - pp.134-141

SIMULATION OF ULTRASONIC FIELDS GENERATED BY SINGLE AND ARRAY TRANSDUCERS THROUGH INTERFACES

Flávio Buiochi
Depto. de Engenharia Mecatrônica da Escola Politécnica da USP, Av. Prof. Mello Moraes, 2231, 05508-900 São Paulo, SP, Brazil.
e-mail fbuiochi@usp.br

Julio Cezar Adamowski
Depto. de Engenharia Mecatrônica da Escola Politécnica da USP, Av. Prof. Mello Moraes, 2231, 05.508-900 São Paulo, SP, Brazil.
e-mail jcadamow@usp.br

Abstract. *This paper presents a computational method for determining reflection and transmission of ultrasonic beams through plane interfaces between elastic media radiated from arbitrary geometry transducers. The ultrasonic field is calculated by the Rayleigh integral method, which is affected by reflection and ttransmission coefficients. The method is divided into two steps. As first step, the velocity potential impulse response is calculated at the interface. In a second step, the reflected and transmitted pressure field is calculated by applying the Huygens' principle to the whole-extended interface. The method is valid for all field regions, and can be performed for any excitation form and array structure. In order to validate the method, a simulated field using a single piston-like transducer is compared to an experimentally measured field through a plane surface between two media (water-acrylic). Moreover, some simulations using an array transducer are performed to present the ability of the computational method to focus acoustic beam through a plane interface considering the first travel time technique on each array element.*

Keywords*: acoustic propagation simulation, ultrasonic field, ultrasonic transducer, array*

1. Introduction

Ultrasonic techniques in nondestructive evaluation (NDE) have mainly been used to detect defects reconstructing 2D or 3D images of the inner part of the components being inspected. Having complex physics involved, the theoretical investigation of the acoustic field produced by a broadband ultrasonic transducer through interfaces is an important tool for typical NDE, because, in most cases, liquid or solid wedges of different geometry exist between the transducer face and the structure. Depending on differences in the acoustic propagation velocity between the discontinued materials, and the specific geometry, significant acoustic beam distortion may occur. For this purpose, a theoretical model is useful to interpret correctly the echographic data obtained by the transmit-receive response from defects. In addition, the model allows the optimization of the main parameters of an inspection system, such as the transducer, coupling material, scanning geometry, etc. Moreover, the extension of simulations to the case of array apertures is of great potential in NDE because it allows the optimization of the beamforming properties of the array. It provides a tool to calculate the optimal focal laws according to the required focus, and to understand the acoustic wave propagation through interfaces.

Different methods have been developed to study the spatial-temporal characteristics of acoustic fields radiated by broadband transducers. One of these methods uses the spatial impulse response to determine the time-dependent pressure at a spatial point (Stepanishen, 1971). The starting point is the Rayleigh integral based on the Huygens' principle, from which each point of a travelling wavefront can be considered as a secondary source of hemispherical disturbance. The acoustic field results from the superposition of hemispherical waves radiated by infinitesimal areas from the transducer. This method, based on the Rayleigh integral and combined with the geometrical optics approximation, can also be used for calculating pressure fields through interfaces (Gengembre and Lhémery, 2000). Other techniques, such as those based on the angular spectrum (Berkhoff *et al.*, 1995), or on finite difference methods (Mast *et al.*, 1997), can also be used for the simulation of acoustic propagation through interfaces. However, these techniques have a high cost of computational time. Moreover, some researchers have implemented ray-tracing techniques as a simplified model to rapidly calculate the beam distortion through interfaces without considering the diffraction effects (Croce *et al.*, 2000).

In this paper, a computational method is presented, which is based on the spatial impulse response (Stepanishen, 1971) and on the discrete representation computational concept (Piwakowski and Sbai, 1999). Both the aperture transducer and the interface are considered as a finite number of elementary sources, each emitting a hemispherical wave. Reflection and transmission fields are taken into account separately and, if the medium is a solid, both longitudinal and transversal components can be calculated separately by the Rayleigh integral. The conversion mode is included in the method considering the incident beam at the interface as a plane wave. Furthermore, the method is extended for the case of array apertures.

2. General description of the method

Consider a source with an arbitrary plane surface S_a embedded in an infinite rigid baffle that is in contact with a medium 1 (Fig. 1). The acoustic pressure field radiated in an isotropic medium can be calculated in the time domain from the Rayleigh integral (Stepanishen, 1971):

$$p(\vec{r}_i,t)=\frac{\rho_1}{2\pi}\frac{\partial}{\partial t}\int_{S_a}\frac{v_n(\vec{r}_a,t-r_{ai}/c_1)}{r_{ai}}dS_a \tag{1}$$

where $p(\vec{r}_i,t)$ is the incident acoustic pressure at the interface before the interaction with it; ρ_1 and c_1 are, respectively, the density and propagation velocity of medium 1; r_{ai} is the distance from the elementary area dS_a located at $\vec{r}_a$ to the point located at $\vec{r}_i$; S_a indicates the surface of the radiating aperture; and $v_n(\vec{r}_a,t)$ is the normal velocity in each point of the aperture.

The planar interface between media 1 and 2 is approximated to a finite-planar interface, which is sufficiently large to intercept the entire radiated field. Now considering that the acoustic pressure $p^{R/T}(\vec{r}_i,t)$ immediately after the interaction of incident waves with the interface is known, it is possible to calculate the reflected and refracted acoustic fields applying the Rayleigh-Sommerfeld integral to the interface considering that it is embedded in an infinite soft baffle:

$$p(\vec{r}_P,t)=\frac{1}{2\pi c_\chi}\int_{S_i}\frac{|\cos(\vec{r}_{iP},\vec{n})|}{r_{iP}}\frac{\partial}{\partial t}p^{R/T}(\vec{r}_i,t-\frac{r_{iP}}{c_\chi})\,dS_i \tag{2}$$

where $p(\vec{r}_P,t)$ is the reflected and transmitted acoustic pressure through the interface; c_χ is the propagation velocity of medium χ, which is 1 for medium 1 (when reflected waves are computed) and 2 for medium 2 (when transmitted waves are computed); r_{iP} is the distance from the elementary area dS_i located at $\vec{r}_i$ to the field point located at $\vec{r}_P$; $\cos(\vec{r}_{iP},\vec{n})$ is the cosine of the angle between the normal vector $\vec{n}$ and the vector $\vec{r}_{iP}$, and its modulus guarantees the use of the same expression in cases of reflection and transmission; and S_i indicates the surface of the finite-plane interface.

The relation between the pressure wave immediately before the interface $p(\vec{r}_i,t)$ and after it $p^{R/T}(\vec{r}_i,t)$ can be approximated by $p^{R/T}(\vec{r}_i,t)=C_M\,p(\vec{r}_i,t)$, where C_{M} represents the reflection and transmission coefficients that are functions of the angle of incidence for the plane wave in medium 1 incident on the interface. Subscript M indicates the wave mode, i.e., it assumes L for longitudinal waves and S for shear waves.

The solution for $p(\vec{r}_P,t)$ presented in Eq. (2) can be further simplified, assuming that the aperture is a uniform piston. Substituting Eq. (1) into (2), and after some calculation, it follows that the transient field is determined by a temporal convolution between the time derivative of the excitation signal $v(t)$ and the velocity potential impulse response $h(\vec{r}_P,t)$ at point P:

$$p(\vec{r}_P,t)=\rho_1\frac{\partial v(t)}{\partial t}*h(\vec{r}_P,t) \tag{3}$$

where the symbol * is the convolution in time, and the velocity potential impulse response at point P is defined by:

$$h(\vec{r}_P,t)=\frac{1}{c_\chi}\int_{S_i}\frac{|\cos(\vec{r}_{iP},\vec{n})|}{2\pi r_{iP}}\frac{\partial}{\partial t}h_a(\vec{r}_i,t-\frac{r_{iP}}{c_\chi})dS_i \tag{4}$$

where $h_a(\vec{r}_i,t)$ is the velocity potential impulse response at a plane which is immediately after the reflected or transmitted waves at the interface during the wave propagation:

$$h_a(\vec{r}_i,t)=C_{\mathrm{M}}\int_{S_a}\frac{\delta(t-r_{ai}/c_1)}{2\pi r_{ai}}dS_a \tag{5}$$

In this work, computations are divided into two parts, using the approach proposed by Piwakowski and Sbai (1999) that is valid for arbitrary apertures. In a first step, after dividing the aperture into a number of elementary surfaces, the velocity potential impulse response $h_a(\vec{r}_i,t)$ is calculated from Eq. (5) at the whole finite-plane interface, which was also approximated by a number of elements of small planar areas. In each of those elements, the impulse response function is affected by the corresponding reflection and transmission coefficients that are assumed constant for a planar interface. In a second step, the velocity potential impulse response $h(\vec{r}_P,t)$ is calculated from Eq. (4) and the reflected and transmitted pressure field is obtained by applying Eq. (3) at every field point P.

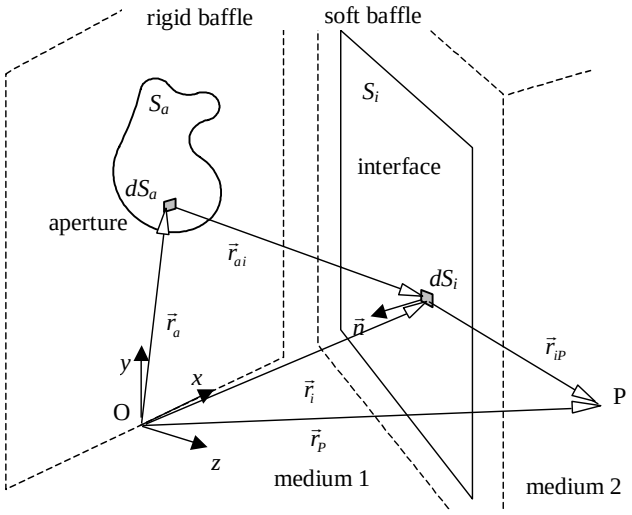

Figure 1. Geometry used to calculate the field produced by an arbitrary source through a plane interface, representing a general case in which the aperture is not parallel to the interface.

3. Array model

The method previously described can easily be adapted to arrays of arbitrary geometry introducing in the equations the time delays and apodization factors that control the ultrasonic beamforming. The closed-form expression of the array model that simulates the transmitted and reflected fields is shown below, and may be applied to 1D or 2D arrays.

Figure 2 depicts the geometry used to calculate the acoustic pressure field generated by an N-element linear array through a planar interface. The pressure field $p(\vec{r}_p,t)$ at a spatial point $\vec{r}_p$ can be obtained from Eqs. (3) and (4), considering that the array impulse response in each of the point of the interface $h_a^{ARRAY}(\vec{r}_i,t)$, is calculated by superimposing the impulse response $h_a^e(\vec{r}_i,t)$ of every array element *e*:

$$h_a^{ARRAY}(\vec{r}_i,t)=\sum_{e=1}^{N} A^e h_a^e(\vec{r}_i,t-T^e) \tag{6}$$

where *N* is the number of array elements, A^e is the apodization factor, and T^e the excitation delay of the eth element. The element impulse response $h_a^e(\vec{r}_i,t)$ immediately after the reflected or transmitted waves at the interface is obtained by integrating over the radiating surface S_a^e of each array element, as defined by Eq. (5), i.e.:

$$h_a^e(\vec{r}_i,t)=C_{\mathrm{M}}\int_{S_a^e}\frac{\delta(t-r_{ai}^e/c_1)}{2\pi r_{ai}^e}dS_a^e \tag{7}$$

Note that it is again based upon Huygen's principle, which states that each array element is approximated by a finite number of elementary areas dS_a^e radiating hemispherical waves, and contributing to the pressure at the interface.

4. Focal law

The beam generated by an array is focused at a spatial point F if all central pulses arrive at F exactly in coincidence, so that the time delays are calculated to compensate for the path differences:

$$T^e = K - t^e \tag{8}$$

where t^e is the propagation time from the focal point F to the central point C^e of the e[th] element and K is a constant that makes all the focusing delays ($K \geq \max\{t^e\}_{e=1,2...\mathrm{N}}$) positive.

If the acoustic propagation velocity of both media, and the geometric position of the array and the interface are known, the minimum propagation time from F to C^e can be determined by considering Snell law. However, an analytical solution for t^e is not attained. A numerical procedure is then desirable, which also has the advantage of being valid for arbitrary geometry of the array and of the interface including non-planar ones. As an example to visualize how the focal law is determined, the N-element linear array as in Fig. 2 can be considered. Specifically, the propagation way from *F* in medium 2 through a planar interface to the center of an array element *e* in medium 1 is shown. It is supposed that an acoustic source, located at the focal point F, generates a hemispherical wave that propagates back to the interface.

The travel time measured is determined by the minimum propagation time of waves arriving from focal point through all point at the interface to the center of each array element *e*, i.e.:

$$t^e = \min\{r_i^{\mathrm{C}^e}/c_1 + r_i^{\mathrm{F}}/c_\chi\}_{i=1,2,...\mathrm{m}}, \qquad \text{for } e = 1,2,\ldots\mathrm{N}, \tag{9}$$

where m is the number of discretized areas at the interface, and r_i^{F} is the distance from the elementary area dS_i located at $\vec{r}_i$ to the focus F, and $r_i^{\mathrm{C}^e}$ is distance from the center of the e[th] element located at C^e to the same elementary area dS_i

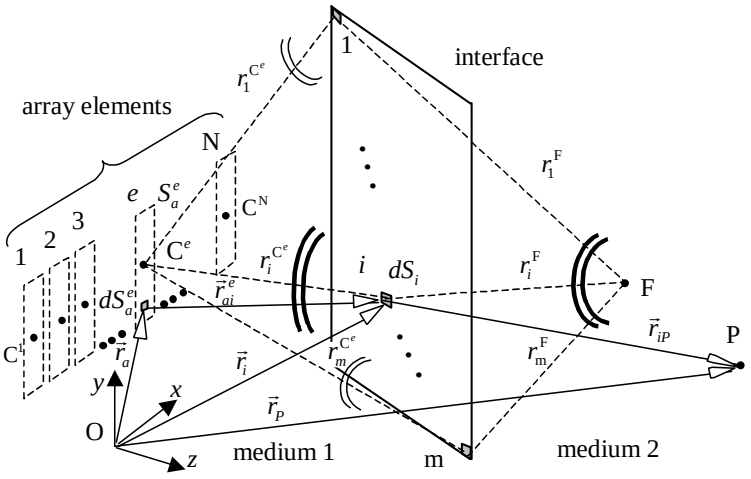

Figure 2. Geometry used to calculate the acoustic field produced by an array through a plane, and the minimum travel time from point F to the center point C^e of any array element.

5. Experimental and simulated comparisons

Experiments to measure the acoustic field through solid interfaces were performed to test the validity of the computational method. A circular transducer with a diameter of 19 mm, which vibrates with a central frequency of 1 MHz and a bandwidth of 50% was used. Simulations require the knowledge of the excitation signal $v(t)$, which was measured facing a needle hydrophone close to approximately 2mm the transducer emitting face.

The measurement system consists of a usual wide band excitation and receiving electronics system, together with an automatic scanning tank. All measurements were carried out in water ($\rho = 1000\,\mathrm{kg/m^3}$, $c_L = 1500\,\mathrm{m/s}$) employing a 0.2-mm-diam hydrophone to measure the acoustic field, and the solid medium is acrylic ($\rho = 1180\,\mathrm{kg/m^3}$, $c_L = 2700\,\mathrm{m/s}$, $c_S = 1400\,\mathrm{m/s}$), where subscripts L and S in the propagation velocity refer to longitudinal and shear waves, respectively. Two physical arrangements were used, which are illustrated in Fig. 3. Each interface is assumed to have an angular orientation α and is located at an axial distance *Z* from the center of the circular transducer (point O). To show the transmitted and reflected acoustic waves, the referential $\mathrm{O}'\bar{x}\,\bar{z}$ for the acrylic-water interface (Fig. 3.a.) and the referential $\mathrm{O}\,x\,z$ for the water-acrylic interface (Fig. 3.b) were adopted, respectively.

Figure 4 shows the images of the maximum pressure distribution for the experimental and simulated refracted waves through the acrylic-water interface for an angle of incidence $\alpha = 15°$ and axial distance $Z = 17\mathrm{mm}$. In this figure, a

thick horizontal line represents the interface position. Figure 5 compares the experimental and computational beam profiles of the refracted field described in Fig. 4 at three different values of coordinate $\bar{z}$: 4mm, 40mm and 76mm. The pressure amplitude was normalized by the maximum value recorded on $\bar{z} = 40\text{mm}$. The coordinate system $O'\bar{x}\,\bar{z}$ (see Fig. 3.a) was considered to show the transmitted pressure amplitude.

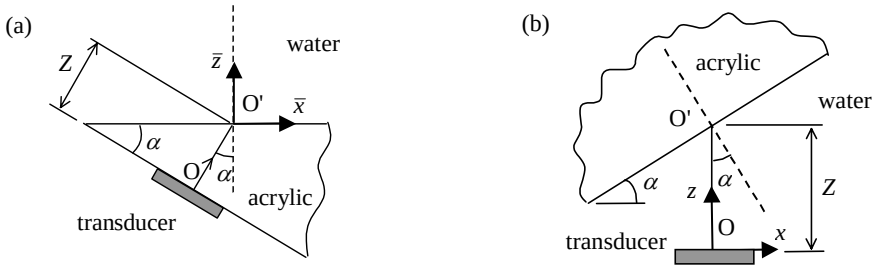

Figure 3. The geometry and the incident wave at an angle α on (a) the acrylic-water and (b) water-acrylic interfaces.

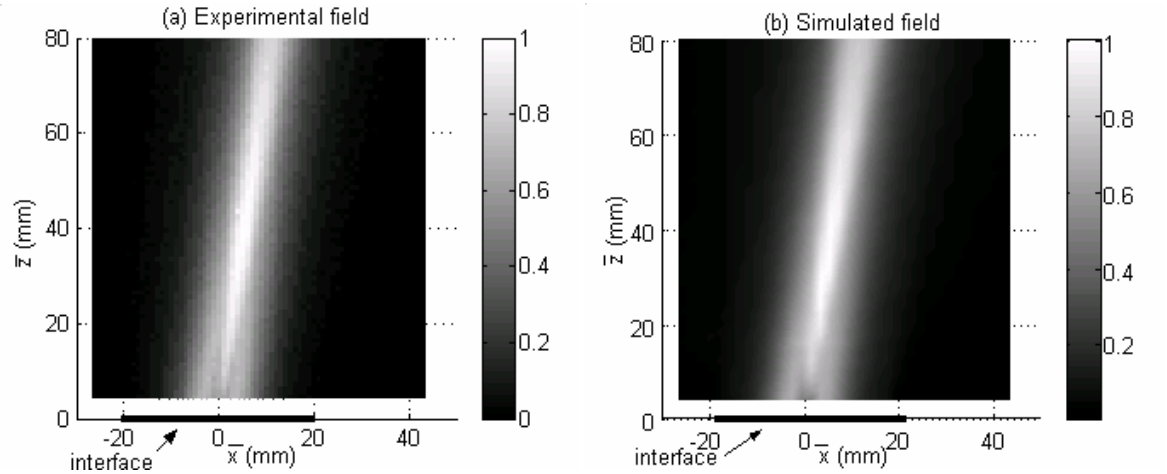

Figure 4. The experimental and simulated fields for α=15º on the acrylic-water interface.

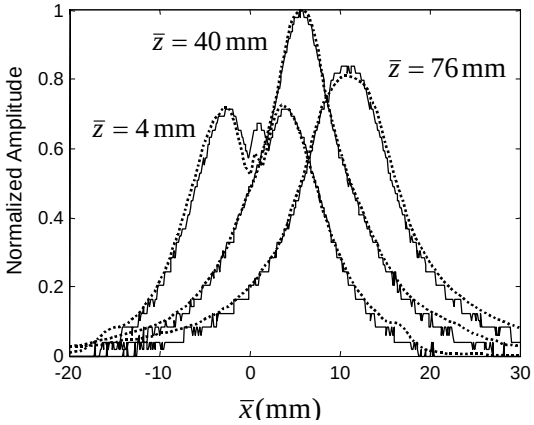

Figure 5. Comparison of experimental (—) and computational (. . . .) data for an angle of incidence α=15º on the acrylic-water interface.

The experimental and simulated reflected fields for the angle of incidence α=30º and axial distance $Z = 30\text{mm}$ on the water-acrylic interface are illustrated in Fig. 6. In this figure, both interface and transducer used in the simulation are represented graphically. Figure 7 shows the beam profile concerning the reflected field at three different values of coordinate *x*: 16mm, 48mm and 80mm. The coordinate system $O\,x\,z$ (see Fig. 3.b) was considered to show the pressure amplitude, which was normalized by the maximum value recorded on $x = 48\text{mm}$.

From Figs. 4 to 7, it is observed that the simulated results are in good agreement with the measured ones for beam profiles and acoustic fields.

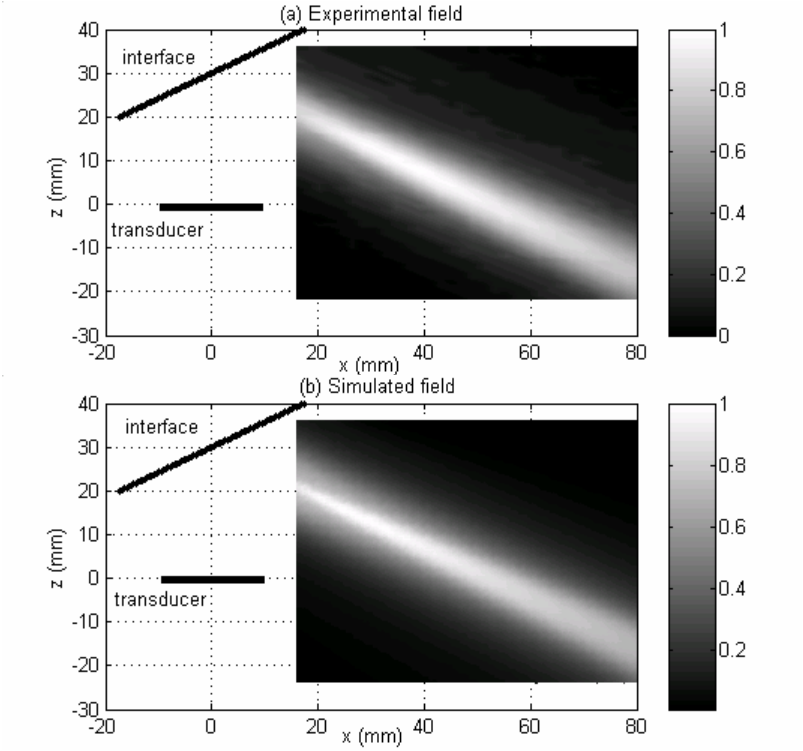

Figure 6. The experimental and simulated fields for α=30º on water-acrylic interface.

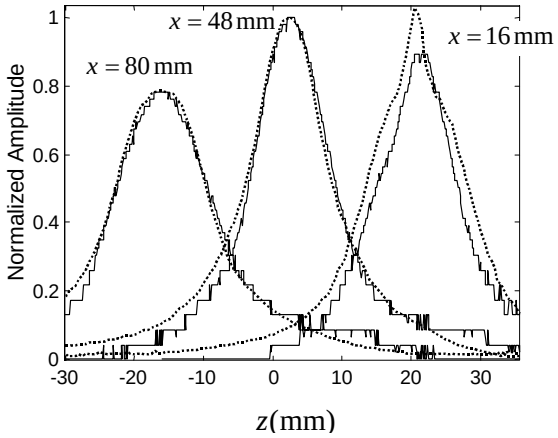

Figure 7. Comparison of experimental (—) and computational (. . . .) data for an angle of incidence α=30º on the water-acrylic interface.

6. Array simulated fields

In order to show the implementation of the computational method for the case of a planar array aperture, it considers an array with 16 rectangular elements, 1.5mm wide and 15mm long, which are separated by gaps of 0.05mm. The radiating surface of each array element emits a temporal excitation of 2-MHz sine-wave single cycle. The simulations were carried out taking medium 1 as acrylic (λ_1=1.35mm) and medium 2 as steel (λ_2=2.95mm), with longitudinal velocities of 2700m/s and 5900m/s, respectively. Two angular orientations ($\alpha = 0^o$ and 25^o) and an axial distance (Z=15mm) define the positions of the rectangular interface of dimensions 26×20 mm relative to referential $Oxyz$ located in the center of the array. The array is similar to those used for NDE of steel structures using acrylic wedges.

Figures 8.a and 8.b show the transmitted simulated fields, respectively, using the 0^o and 25^o interfaces, being the array focused at X=5, Y=0, and Z=30mm. For these simulations, only longitudinal waves were considered, and the transmission and reflection coefficients were assumed to be constant (C_M = 1).

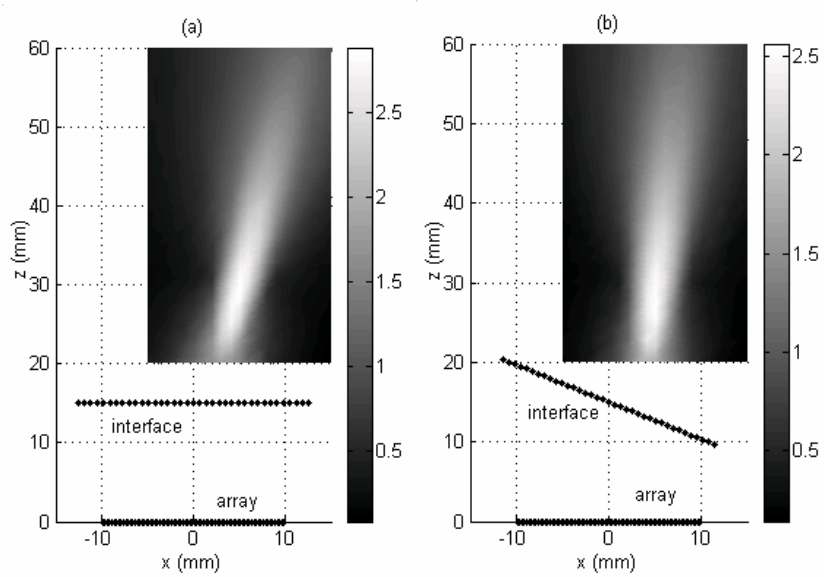

Figure 8. Simulations of the acoustic field generated by a phased array through the parallel interface (a), and through the inclined interface (b). In both cases the array is focused at the point (X=5, Y=0, and Z=30mm).

Figure 9 shows the focal laws for the two different cases presented in Fig. 8, using a normalized time delay ($c_1 t$) defined by the product between propagation velocity of medium 1 (c_1) and delay time (t). The results presented in Fig. 9 demonstrate that the above method of focal laws calculation is useful for acoustic beamforming through interfaces, using the first travel time on each center of the array element. Furthermore, this figure shows that the computational method can easily be applied to simulate the transmitted and reflected acoustic fields radiated by arrays.

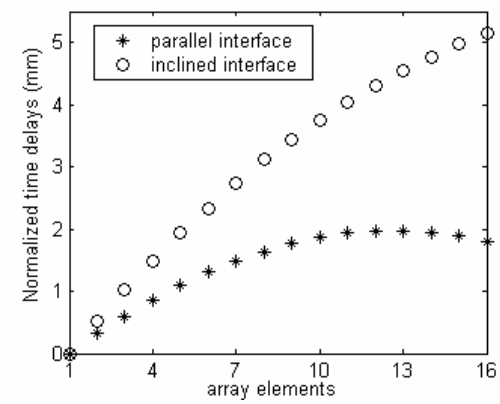

Figure 9. The normalized time delays calculated by the geometry solution for two cases: parallel and 25^o inclined interfaces to the array face.

As equation (5) provides a means of predicting the acoustic field at any instant and any spatial point, the transient ultrasonic wave propagation can be determined. Figure 10 shows temporal pressure fields at four normalized propagating times ($c_1 t = 21$, 23, 25, and 27mm) with the longitudinal velocity of medium 1 for the case of Fig. 8.a. In this simulation, we presented the reflected and transmitted waves, and it can be noticed that there are no coherent reflected waves, because the focal point is in the transmitted field.

7. Conclusions

A computational method was presented for the calculation of the reflected and transmitted field generated by transducer of arbitrary shape through a planar interface. The method can also handle transducer arrays. The field is determined by the Rayleigh integral, which is applied first to the radiated beam from the aperture and later to the reflected and to the transmitted beam from the interface. It was verified that if the transducer aperture and the interface are discretized with a large number of small area elements, the computational time increases. Experiments made using a circular transducer and a planar interface show that there is a good agreement between experimental and theoretical results. Linear arrays development has been conducted in our lab, however, experimental results have not been obtained yet to be compared with simulation results. Although the examples presented in this work are specified to linear arrays,

the computational method developed here can easily be extended to 2D arrays. The simulations proved that the computational method is an important tool to calculate the beam and to analyze focal laws through interfaces applied in NDE.

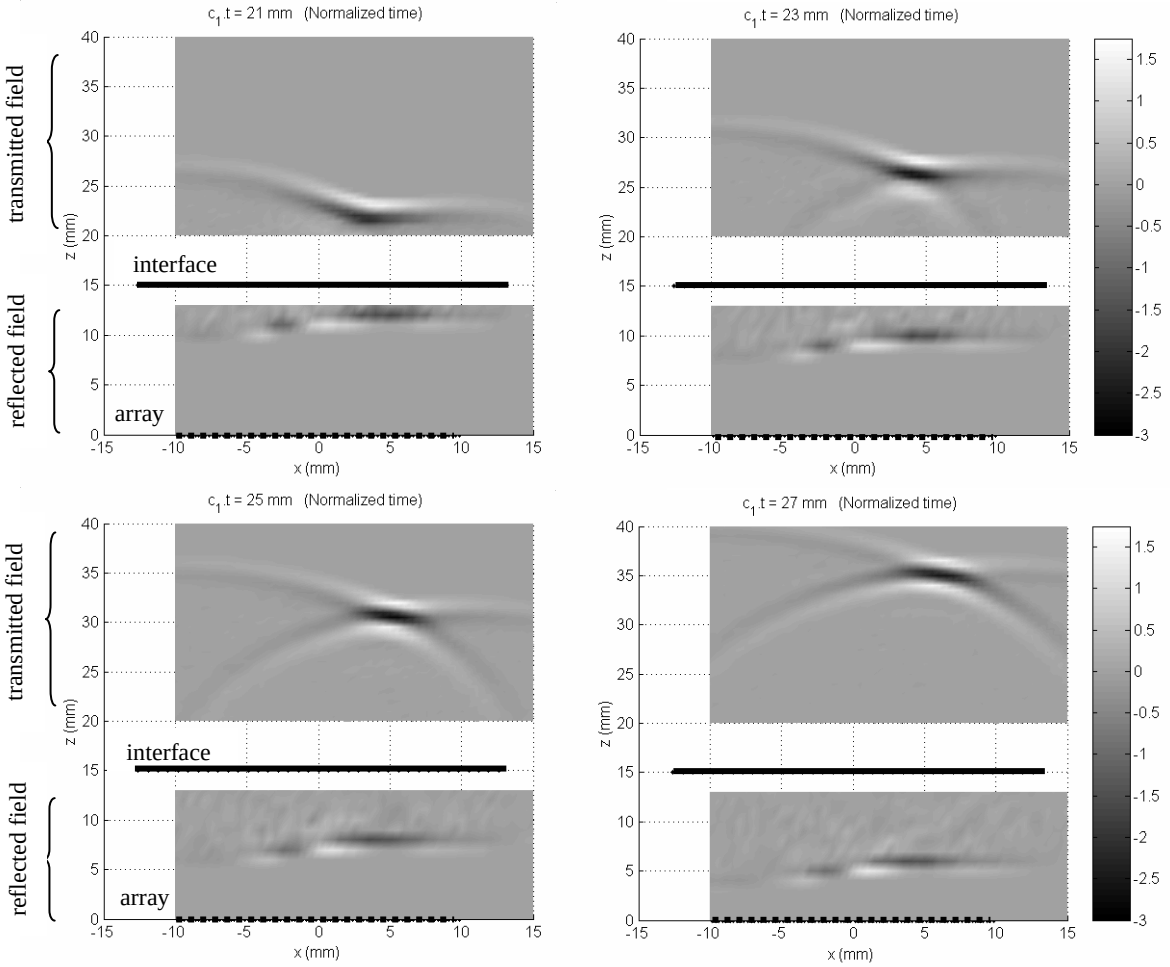

Figure 10. Ultrasonic wave propagation at normalized time (related to c_1): (a) 21mm, (b) 23mm - both in the near field -, (c) 25mm - approximately at focus -, and (d) 27mm - in the far field -.

8. Acknowledgements

The authors would like to thank FAPESP, CNPq, FINEP/ CTPETRO - Brazil for funding this research program.

9. References

Berkhoff, A.P., van den Berg, P.M. and Thijssen, J.M., 1995, "Iterative calculation of reflected and transmitted acoustic waves at a rough interface", IEEE Trans. Ultrason., Ferroelect., Freq. Contr., Vol. 42, No. 4, pp. 663-671.

Croce, R., Calmon, P. and Paradis, L., 2000, "Modeling of propagation and echo formation in a multilayered structure" Ultrasonics, Vol. 38, pp. 537-541.

Gengembre, N. and Lhémery, A., 2000, "Calculation of wideband ultrasonic fields radiated by wate-coupled transducers into heterogeneous and anisotropic media", in D.O. Thompson and D.E. Chimenti (eds.), Review of Progress in QNDE, Plenum Press, New York, Vol. 19, pp. 977-984.

Mast, T.D., Sparrow, V.W. and Waag, R., 1997, "Simulation of ultrasonic pulse propagation through the abdominal wall", J. Acoust. Soc. Am., Vol. 102, pp. 1177-1190.

Piwakowski, B. and Sbai. K., 1999, "A new approach to calculate the field radiated from arbitrarily structured transducer arrays", IEEE Trans. Ultrason., Ferroelect., Freq. Contr., Vol. 46, No. 2, pp. 422-439.

Stepanishen, P.R., 1971, "Transient radiation from piston in an infinite planar baffle", J. Acoust. Soc. Am., Vol. 49, pp. 1629-1638.

10. Responsibility notice

The authors are the only responsible for the printed material included in this paper.